Nanocomposite Fluid

DOI: 10.1002/anie.201001398

Synthesis of Transparent and Field-Responsive $BaTiO_3$ Particle/Organosiloxane Hybrid Fluid

*Ken-ichi Mimura, Yuki Nishimoto, Hiroshi Orihara, Makoto Moriya, Wataru Sakamoto, and Toshinobu Yogo**

Nanocomposite fluids attract special attention because of their high thermal conductivities, which are applied in electronics, micro- and nanoelectromechanical systems, and other heat-transport devices.[1,2] Nanocomposite fluids are synthesized by mixing nanoparticles synthesized separately as a dry powder and a fluid. However, uniformly mixing nanoparticles and fluids is difficult because nanoparticles form agglomerates as a result of van der Waals forces. The change in aggregation with changes in anisotropy appears to be one of the reasons for inconsistent and nonreproducible thermal conductivity data.[3] Chemical synthesis of nanoparticles in solution is one of the most advantageous methods for synthesis of nanocomposite fluids. Nanoparticle synthesis by controlled precursor hydrolysis is meritorious because nanoparticles of uniform size are formed.[4] In addition, nanoparticles can be stabilized through steric repulsion between chemically bound polymers on the particle surfaces.[5]

Smart materials produce a useful effect in response to external stimuli such as strain, stress, temperature, pH, and electric and magnetic fields.[6] Electrorheological (ER) fluids are smart materials whose rheological properties change on exposure to an external electric field.[7] A heterogeneous ER fluid, which consists of particulate dispersoid and liquid, behaves as a Bingham fluid under an applied electric field and shows yield stress.[8] However, heterogeneous ER fluids exhibit problematic particle sedimentation, which leads to changes in fluid properties and dielectric breakdown. Barium titanate ($BaTiO_3$, BT) displays excellent ferroelectricity, piezoelectricity, and a high dielectric constant.[9] It has a high tolerance to dielectric breakdown because of its high dielectric constant, and this makes BT particles an appropriate dispersoid for ER fluids. $BaTiO_3$ nanoparticles have been synthesized by various methods, such as precipitation,[10] sol–gel process,[11] hydrothermal/solvothermal synthesis,[12] pyrolysis of a bimetallic alkoxide precursor,[13] composite-hydroxide-mediated approach,[14] and liquid–solid–solution phase transfer.[15] $BaTiO_3$ nanoparticles synthesized by hydrolysis of a Ba–Ti double alkoxide were used in heterogeneous ER fluid.[16] Nanoparticle-based hybrid fluids display many advantages applicable to ER fluids, such as low density, better stability against sedimentation, and low wear of the fluid vessel. However, no optical properties have been reported for perovskite-based fluids because of their nontransparency to visible light. To synthesize transparent fluids, the interface between the nanoparticles and the base fluid must be modified with appropriate organics. The interface can be designed to display polarizability in an external field and thus yield stimuli-responsive materials. Here we report the synthesis of transparent fluid incorporating perovskite $BaTiO_3$ particles by a chemical process. The fluid shows field-responsive rheological behavior and optical transmittance.

Figure 1 a shows the molecular structure of dimethylsiloxane derivative **1** bearing carbinol side chains $[MeSi(R'OH)]_m$. The BT nanoparticle/organosiloxane hybrid fluid was synthesized by hydrolyzing the Ba–Ti precursor with 30 equiv H_2O and subsequent reaction with siloxane **1**. The hydrolysis product, before reaction with siloxane **1**, gave several crystal diffraction peaks which were in accordance with perovskite $BaTiO_3$ (JCPDS card No. 05-0626, Figure S1a in Supporting Information). The XRD pattern of the fluid showed several

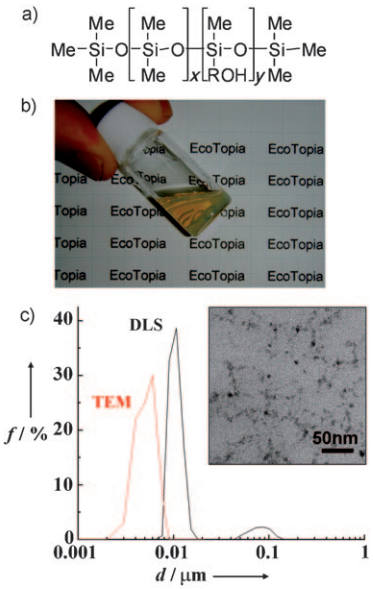

Figure 1. a) Molecular structure of siloxane **1**. b) Appearance of $BaTiO_3$ particle/siloxane fluid (fluid **1**). c) Microstructure and size distribution of $BaTiO_3$ particles in fluid **1** by TEM and DLS.

[*] K. Mimura, Dr. M. Moriya, Dr. W. Sakamoto, Prof. T. Yogo
Division of Nanomaterials Science, EcoTopia Science Institute, Nagoya University
Furo-cho, Chikusa-ku, Nagoya 464-8603 (Japan)
Fax: (+81) 52-789-2121
E-mail: yogo@esi.nagoya-u.ac.jp
Y. Nishimoto, Prof. H. Orihara
Department of Applied Physics, Graduate School of Engineering, Hokkaido University
Kita 13, Nishi 8, Kita-ku, Sapporo 060-8628 (Japan)

Supporting information for this article is available on the WWW under http://dx.doi.org/10.1002/anie.201001398.

diffraction peaks and a broad peak around $2\theta = 12°$ (Figure S1b), which correspond to $BaTiO_3$ and siloxane **1**, respectively. The crystallite size of the $BaTiO_3$ nanoparticles obtained by hydrolysis with 30 equiv H_2O was calculated to be about 5.5 nm by using the Scherrer equation.

The appearance of BT/30 H_2O/3 $[MeSi(R'OH)]_m$ hybrid fluid **1** is shown in Figure 1b. Fluid **1** is highly transparent. Its refractive index of 1.42 at 25 °C is slightly higher than that of the base siloxane ($n = 1.41$ at 25 °C). Since the refractive index of single-crystal $BaTiO_3$ ($n \approx 2.4$) is higher than that of base siloxane **1**, the refractive index of the hybrid fluid increased on incorporation of BT nanoparticles. Figure 1c shows the microstructure of fluid **1** observed by transmission electron microscopy (TEM). The TEM image shows monodisperse BT particles with an average size of 5.75 nm, are in good agreement with the crystallite size estimated by using the Scherrer equation. The size distribution of BT nanoparticles dispersed in fluid **1**, measured by dynamic light scattering (DLS), is also displayed in Figure 1c. The DLS measurements show that more than 90 % of the BT nanoparticles have a size distribution ranging from 7 to 15 nm. The larger particles (10 %) appeared to be secondary aggregates in fluid **1**, because the monodispersity of the particles was confirmed by TEM. The median diameter D_{50} and 90 % frequency diameter D_{90} were 9.7 and 14.1 nm, respectively. Measurements of BT nanoparticle size by DLS and TEM indicate that the BT nanoparticles are bound to siloxane **1** in the fluid.

Chemical interactions between the BT particles and the base fluid were investigated by IR spectroscopy. Siloxane **1** shows an absorption band at 3460 cm^{-1} assigned to OH (Figure S2a). When **1** reacted with $BaTiO_3$ nanoparticles synthesized by hydrolysis, the 3460 cm^{-1} band disappeared in the IR spectrum of the BT/30 H_2O/$[MeSi(R'OH)]_m$ hybrid gel powder (Figure S2b). This suggests that siloxane **1** is chemically bound to BT nanoparticles through OH groups, affording M-O-R-Si bonds (R: organic groups, M: Ba or Ti). When the molar ratio between $[MeSi(R'OH)]_m$ and BT was 1.0, the product was a transparent gel. When the ratio was increased to 3.0, the product was a transparent fluid (fluid **1**). In addition, the OH band shown in Figure S2c was almost the same as for siloxane **1**. Because of the molar excess of siloxane with respect to BT, a large number of free OH terminal groups of siloxane **1** remain in the transparent fluid **1**. Hence, no difference in OH absorption was observed between fluid **1** and siloxane **1**.

The ^1H and ^{13}C NMR spectra of siloxane **1** were compared with those of BT/30 H_2O/x $[MeSi(R'OH)]_m$ hybrids. The NMR data showed the R′ side chain in $[MeSi(R'OH)]_m$ be $-(CH_2)_3O(CH_2)_2OH$ (Figures S3a and S4a).[17] The signal marked with an arrow at $\delta_H = 1.91$ ppm, which corresponds to an OH proton (Figure S3a), disappeared in the spectrum of the hybrid fluid (Figure S3b). This suggests that siloxane **1** is chemically bound to BT nanoparticles. Also, the signal at $\delta_C =$ 62.0 ppm attributed to the OH-bearing carbon atom in the BT/30 H_2O/$[MeSi(R'OH)]_m$ hybrid gel (Figure S4b) showed a downfield shoulder (marked with an arrow), which was assigned to the carbon atom of the CH_2O–M bond resulting from the converted terminal OH group. This also indicates that siloxane **1** is chemically bound to the BT nanoparticles through the OH groups by formation of M–$(ORSi)_n$ bonds (R: organic groups, M: Ba or Ti). The presence of chemically bound siloxane on BT particles results in larger particles in the fluid, as confirmed by DLS. Therefore, BT particles are stabilized by steric repulsion between siloxane molecules attached to the particle surfaces. The siloxane polymer prevents nanoparticle agglomeration and thus leads to a transparent fluid.

Figure 2a shows shear stress versus shear rate curves for fluid **1** under various dc fields. For comparison, fluid **2** was synthesized from Ba–Ti alkoxide and dimethylsiloxane derivative $(Me_2SiO)_nR''OH$ (**2**) under the same synthetic conditions. Siloxane **2** has only one terminal OH group in its molecular structure (Figure S5). In the absence of a dc field, both hybrid fluids display Newtonian behavior characterized by a linear relation between shear rate and shear stress (Figure 2a and Figure S5). When the electric field was applied to fluid **2**, little change in shear stress was observed (Figure S5). In contrast, fluid **1** behaved as a pseudoplastic fluid under the applied field, and a nonlinear relationship became dominant above 3 kV mm^{-1}. This difference in behaviors is attributed to the different numbers of OH groups in siloxanes **1** and **2**. Siloxane **1** has a large number of side-chain OH groups that can be bound to BT particles. Thus, BT nanoparticles are strongly bound to siloxane **1**, and interactions between particles and polymeric surfactant are strong (Figure S6). On the other hand, siloxane **2** has only one OH group per siloxane, which results in only weak inter-

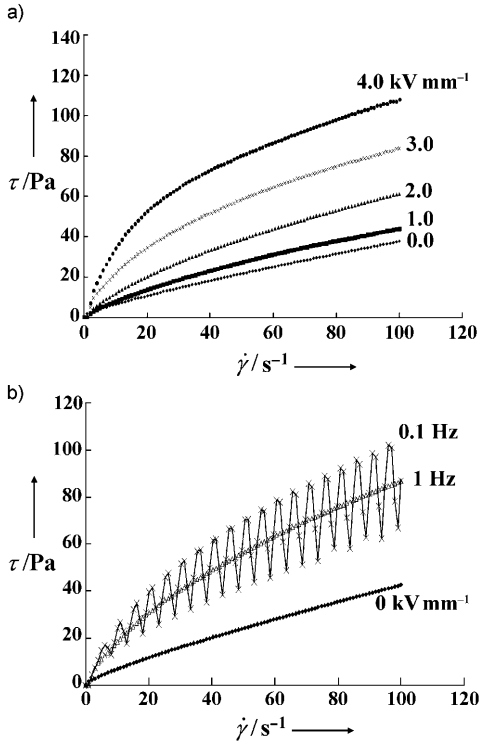

Figure 2. a) Shear stress/shear rate curves for fluid **1** in dc fields from 0 to 4.0 kV mm^{-1}. b) Shear stress/shear rate curves for fluid **1** in ac fields of 0.1 and 1.0 Hz and at 0 and 4.0 kV mm^{-1}.

actions between nanoparticles and **2**. This difference in number of OH groups produces a different response of BT nanoparticles on application of an electric field. Increasing the amount of $BaTiO_3$ particles in the fluid increases the yield stress.[16b] However, the fluid loses its transparency at higher contents of $BaTiO_3$ particles. Thus, the dispersion properties must be much improved in the future.

Figure 2b shows shear stress versus shear rate curves for fluid **1** under sinusoidal ac fields at $\pm 4\,kV\,mm^{-1}$. When a 0.1 Hz ac field was applied to the hybrid fluid, the repeated increase and decrease in shear stress gave a sine-like curve (Figure 2b). This increase and decrease in shear stress occurred when the applied field was changed from positive to negative and vice versa. The chainlike particle alignment between electrodes induced by the electric field is the origin of the increase in shear stress. Depending on the change in ac electric field, BT nanoparticles move along the direction of the electric field, and this movement resists shear because the direction of motion of the BT nanoparticles is perpendicular to the shear direction in the rotating plates of the rheometer. At 1.0 Hz, the absence of a sine-like change in the shear stress/shear rate curve suggests that particle motion does not follow the polarity changes at this frequency.

Figure 3a shows the UV/Vis spectra of fluid **1** sandwiched between silica glass plates coated with indium tin oxide (ITO) under a dc field. Fluid **1** displays high transmittance under visible light in the absence of a dc field. The transmittance of fluid **1** decreased at stronger applied fields. This decrease in transmittance is larger for fluid **1** than for fluid **2** (Figure S7). At $4\,kV\,mm^{-1}$, the transmittance at 589 nm decreased by 66% compared to that at zero field. The reason for this decrease may be that attraction of BT nanoparticles toward the electrode under the applied electric field causes their density on the electrode plate to increase locally. The nanoparticles, which are temporarily agglomerated around the electrode plate, scatter and reflect the incident light, reducing the transmittance of the hybrid fluid. Figure 3b shows the UV/Vis spectra of fluid **1** and siloxane **1** sandwiched between ITO-coated silica glass plates. The arrows indicate the on and off positions of the electric field. Under an applied dc field, the transmittance of the hybrid fluid decreased immediately to about 78%, and then gradually to about 62% after 300 s in the on position. In contrast, the transmittance of siloxane **1** showed no change under the electric field. The transmittance of fluid **1** recovered to 90% about 200 s after the field was turned off. Under a $4.0\,kV\,mm^{-1}$ rectangular ac field, the transmittance first decreased to about 86%, and then repeated increases and decreases in transmittance were observed in response to the field (Figure S8). The significant changing points in transmittance (Figure S8) corresponded to points where the polarity of the field was switched from positive to negative and vice versa. These results confirm field-responsive motion of BT nanoparticles in the hybrid fluid.

Figure 4a shows the change in sheer stress for fluid **1** as a function of time under a $4.0\,kV\,mm^{-1}$ applied dc field at a constant shear rate of $2\,s^{-1}$. When the dc field was applied to fluid **1**, the stress increased rapidly to 15 Pa within 2 s and decreased to 10 Pa after 5 s, before increasing gradually to 13 Pa at 40 s. The dynamic behavior of fluid **1** was monitored under constant shear by using a confocal scanning laser microscope developed by us.[18] The observed volume was $167 \times 88 \times 100\,\mu m$ from the bottom ITO electrode. The white

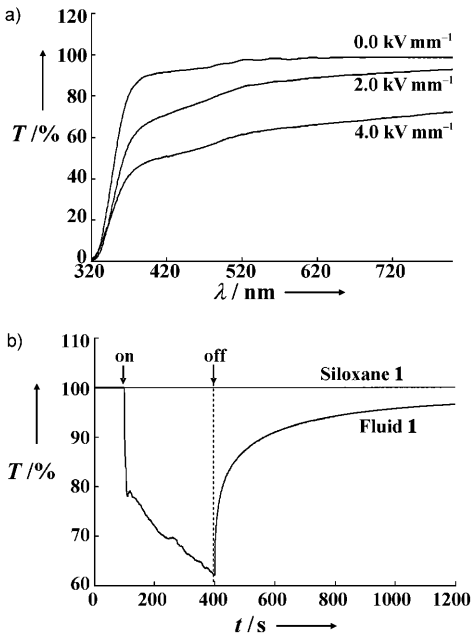

Figure 3. Changes in transmittance with dc field for $BaTiO_3$ particle/siloxane hybrid fluid. a) Change in transmittance of fluid **1** in dc fields of 0–4.0 $kV\,mm^{-1}$. b) Change in transmittance at 589 nm with on–off switching of a 4.0 $kV\,mm^{-1}$ dc field.

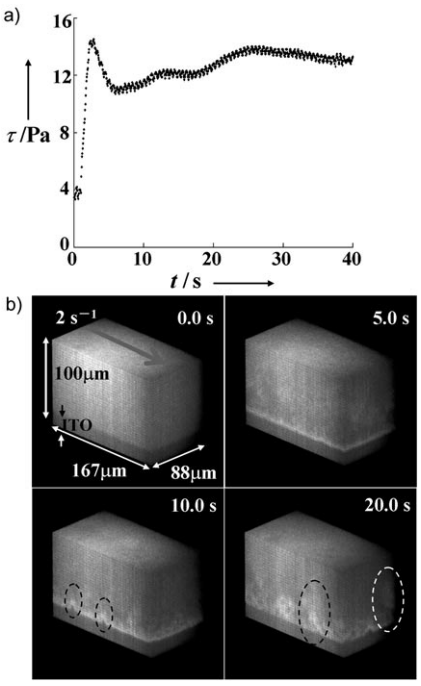

Figure 4. Shear stress versus time curve and 3D images constructed by confocal fluorescence microscopy for fluid **1**. a) Stress versus time curve at constant shear rate of $2\,s^{-1}$. b) 3D images at 0.0, 5.0, 10.0, and 20.0 s, which correspond to the times shown in (a).

dots in Figure 4b correspond to fluorescence from BT nanoparticles modified with fluorescein. The first increase in stress corresponds to rapid movement of particles to the bottom ITO electrode. After 5 s, an aggregated layer of white dots about 4 μm thick was formed on the ITO electrode. Because the polarity of the bottom electrode was negative, the particles were positively charged. From 10 to 40 s, the layered particles were disturbed by shear and redispersed in the fluid, as shown by dashed ellipses in Figure 4b. The white dots formed an aligned structure perpendicular to the electrodes from 25 to 40 s (Figure S9). Similarly, the changes in optical transmittance shown in Figure 3 and Figure S8 of the Supporting Information result from the motion of BT nanoparticles in the fluid under the field.

The dielectric constant of fluid **1** was slightly higher than that of the base fluid (Figure S10), because BT nanoparticles with high dielectric constant were incorporated in fluid **1**. The composite dielectric constant for spherical inclusions in a continuous matrix is expressed by Maxwell's equation (1)[19]

$$\varepsilon_{\text{fluid}} = \varepsilon_{\text{siloxane}} \frac{\varepsilon_{\text{BT}} + 2\varepsilon_{\text{siloxane}} - 2\phi_{BT}(\varepsilon_{\text{siloxane}} - \varepsilon_{\text{BT}})}{\varepsilon_{\text{BT}} + 2\varepsilon_{\text{siloxane}} + \phi_{BT}(\varepsilon_{\text{siloxane}} - \varepsilon_{\text{BT}})} \quad (1)$$

where $\varepsilon_{\text{fluid}}$, ε_{BT}, and $\varepsilon_{\text{siloxane}}$ are the dielectric constants of the hybrid fluid, BT nanoparticles, and base siloxane, respectively, and ϕ_{BT} is the volume fraction of BT nanoparticle; ε_{BT} was assumed to be about 200 for BT nanoparticles,[20] $\varepsilon_{\text{fluid}}$ is 3.62 from the average value measured from 10^2 to 10^6 Hz for the base siloxane, and ϕ_{BT} was calculated from the molar ratio of BT to siloxane **1** (1/3) and the densities (6.02 g cm^{-3} for BT calculated by using JCPDS card No. 05-0626, 0.975 g cm^{-3} for siloxane **1**). The dielectric constant was estimated as 3.76 for hybrid fluid **1**, in good agreement with the measured value (about 3.81). Dielectric constant and loss of base siloxane **1** were almost independent of frequency (Figure S10), while the dielectric constant and loss of the hybrid fluid are frequency-dependent, especially increasing for frequencies ranging below 100 Hz. A similar increase in dielectric loss at low frequencies was observed for heterogeneous ER fluid systems. The dielectric loss is attributed to interfacial polarization between BT nanoparticles and the chemically bound organosiloxane derivative. The field-responsive properties are attributed to the interfacial polarization.[21,22]

In conclusion, a transparent $BaTiO_3$ nanoparticle/siloxane hybrid fluid was synthesized from $BaTiO_3$ nanoparticles and dimethylsiloxane derivatives containing OH groups. The transparent and homogeneous fluid is sediment-free and is a smart material which changes its rheological and optical properties in response to an external field. Field-responsive nanocomposite fluids with optical transparency can be expected to have a broad range of applications. A homogeneous nanocomposite fluid can prevent channel clogging, pipeline erosion, and pressure drop. The fluid may act as a novel guest material for emerging optofluidics, a combination of optics and microfluidics.[23] Remotely controlling the concentration gradient of fluids by using an electric field may also be utilized in optofluidics. "True" nanocomposite fluids offer an important experimental basis for nanocomposite fluid science.

Experimental Section

Figure 1a and Figure S5 show the molecular structures of the two dimethylsiloxane derivatives. Siloxane **1** contains carbinol side chains, whereas one terminal alkyl group of siloxane **2** is modified with an OH group. Siloxanes **1** (Shin-Etsu Chemical, X-22-4039, $M = 56000$, functional group equivalent weight: 965.5 g mol^{-1}) and **2** (Chisso, FM-0411) were used as received. Base siloxanes **1** and **2** are abbreviated as $[MeSi(R'OH)]_m$ and $(Me_2SiO)_nR''OH$, respectively. Ethanol and 2-ethoxyethanol (EGMEE, Kishida Chemical) were dried over magnesium ethoxide and molecular sieves, respectively, and distilled before use. Barium metal (Raremetalic, Tokyo, Japan) and titanium tetraisopropoxide ($Ti(OiPr)_4$, Kojundo Chemical) were used as received. Barium metal (0.49 g, 3.59 mmol) was cut into $Ti(OiPr)_4$ (1.02 g, 3.59 mmol) dissolved in ethanol/EGMEE (5/1 v/v, 48 mL). The reaction mixture was heated to reflux at 80 °C for 18 h to produce a clear solution. A Ba–Ti double alkoxide was hydrolyzed by adding CO_2-free water (30 equiv) and heating the mixture to reflux for 24 h to yield a clear solution containing $BaTiO_3$ nanoparticles. Siloxane **1** (10.4 g) was added to the solution, which was then heated at 80 °C for 20 h. The solvent was evaporated in vacuo to give $BaTiO_3$/organo-polysiloxane hybrid fluid **1**. While a clear gel was obtained for BT/30 H_2O/$[MeSi(R'OH)]_m$ hybrid, BT/30 H_2O/3$[MeSi(R'OH)]_m$ hybrid was a transparent viscous fluid. The concentration of $BaTiO_3$ in fluid **1** was 9.0 wt%. Fluid **2** was synthesized from the $BaTiO_3$ nanoparticle solution and siloxane **2** under the same conditions. Characterization methods are provided in the Supporting Information.

Received: March 9, 2010
Published online: June 10, 2010

Keywords: functional materials · nanoparticles · nanotechnology · organic–inorganic hybrid composites · siloxanes

[1] a) S. U. S. Choi, *Developments and Application of Non-Newtonian Flows*, Amer. Soc., Mech. Eng., New York, **1995**, 99; b) S. Lee, S. U. Choi, S. Li, J. Eastman, *J. Heat Transfer* **1999**, *121*, 280; c) J. A. Eastman, S. R. S. R. Phillpot, S. U. S. Choi, P. Keblinski, *Annu. Rev. Mater. Res.* **2004**, *34*, 219.
[2] X. Q. Wan, A. S. Mujumdar, *Int. J. Therm. Sci.* **2007**, *46*, 1.
[3] P. Keblinski, J. A. Eastman, D. G. Cahill, *Mater. Today* **2005**, *8*, 36.
[4] a) H. Goesmann, C. Feldmann, *Angew. Chem.* **2010**, *122*, 1402; *Angew. Chem. Int. Ed.* **2010**, *49*, 1362; b) A.-H. Lu, E. L. Salabas, F. Schüth, *Angew. Chem.* **2007**, *119*, 1242; *Angew. Chem. Int. Ed.* **2007**, *46*, 1222; c) J. A. Dahl, B. L. S. Maddux, J. E. Hutchison, *Chem. Rev.* **2007**, *107*, 2228; d) L. Brus, *Acc. Chem. Res.* **2008**, *41*, 1742.
[5] P. Claessona, E. Poptosheva, E. Blomberga, A. Dedinaite, *Adv. Colloid Interface Sci.* **2005**, *114–115*, 173.
[6] a) M. A. Cohen Stuart, W. T. S. Huck, J. Genzer, M. Muller, C. Ober, M. Stamm, G. B. Sukhorukov, I. Szleifer, V. V. Tsukruk, M. Urban, F. Winnik, S. Zauscher, I. Luzinov, S. Minko, *Nat. Mater.* **2010**, *9*, 101; b) F. Xia, L. Jiang, *Adv. Mater.* **2008**, *20*, 2842; c) Y. Liu, H. Lv, X. Lan, J. Leng, S. Du, *Compos. Sci. Technol.* **2009**, *69*, 2064.
[7] a) T. C. Halsey, *Science* **1992**, *258*, 761; b) T. Hao, *Adv. Mater.* **2001**, *13*, 1847.
[8] W. M. Winslow, *J. Appl. Phys.* **1949**, *20*, 1137.
[9] a) M. Zgonik, P. Bernasconi, M. Duelli, R. Schlesser, P. Günter, M. H. Garrett, D. Rytz, Y. Zhu Y, X. Wu, *Phys. Rev. B* **1994**, *50*, 5941; b) G. Arlt, D. Hennings, G. de With, *J. Appl. Phys.* **1985**, *58*, 1619.

[10] a) G. Fan, L. Huangpu, X. He, *J. Cryst. Growth* **2005**, *279*, 489; b) F. C. M. Woudenberg, W. F. C. Sager, J. E. ten Elshof, H. Verwij, *Thin Solid Films* **2005**, *471*, 134.
[11] J. Qi, L. Li, Y. Wang, Z. Gui, *J. Cryst. Growth* **2004**, *260*, 551.
[12] M. Niderberger, N. Pinna, J. Polleux, M. Antonietti, *Angew. Chem.* **2004**, *116*, 2320; *Angew. Chem. Int. Ed.* **2004**, *43*, 2270.
[13] S. O'Brien, L. Brus, C. M. Murray, *J. Am. Chem. Soc.* **2001**, *123*, 12085.
[14] H. Liu, C. Hu, Z. L. Wang, *Nano Lett.* **2006**, *6*, 1535.
[15] X. Wang, J. Zhuang, Q. Peng, Y. Li, *Nature* **2005**, *437*, 121.
[16] a) T. Yogo, T. Yomamoto, W. Sakamoto, S. Hirano, *J. Mater. Res.* **2004**, *19*, 3290; b) T. Yogo, R. Fukuzawa, W. Sakamoto, S. Hirano, *J. Nanopart. Res.* **2005**, *7*, 633.
[17] R. M. Silverstein, F. X. Webster, D. Kiemle, *Spectrometric Identification of Organic Compounds*, 7th ed., Wiley, New York, **2005**, p. 127, 204.
[18] K. Aida, Y. H. Na, T. Nagaya, H. Orihara, *Phys. Rev. E* **2009**, *80*, 041807.
[19] D. H. Yoon, J. Zhang, B. I. Lee, *Mater. Res. Bull.* **2003**, *38*, 765.
[20] S. Wada, A. Yazawa, T. Hoshina, Y. Kameshima, H. Kakemoto, T. Tsurumi, Y. Kuroiwa, *IEEE Trans. Ultrasonic. Ferroelect. Freq. Control* **2008**, *55*, 1895.
[21] H. Block, J. P. Kelly, A. Qin A, T. Watson, *Langmuir* **1990**, *6*, 6.
[22] J. Umeda, W. Sakamoto, T. Yogo, *J. Mater. Res.* **2009**, *24*, 2221.
[23] a) G. M. Whitesides, *Nature* **2006**, *442*, 368; b) D. Psaltis, S. R. Quarke, C. Yang, *Nature* **2006**, *442*, 381.

